# Finite Area Method for Nonlinear Supersonic Conical Flows

S. S. Sritharan*
*ICASE, NASA Langley Researh Center, Hampton, Virginia*
and
A. Richard Seebass†
*University of Colorado, Boulder, Colorado*

**A fully conservative numerical method for the computation of steady inviscid supersonic flow about general conical bodies at incidence is described. The procedure utilizes the potential approximation and implements a body conforming mesh generator. The conical potential is assumed to have its best linear variation inside each mesh cell; a secondary interlocking cell system is used to establish the flux balance required to conserve mass. In the supersonic regions the scheme is desymmetrized by adding artificial viscosity in conservation form. The algorithm is nearly an order of a magnitude faster than present Euler methods and predicts known results accurately and qualitative features such as nodal point liftoff correctly. Results are compared with those of other investigators.**

## Introduction

CONICAL flows are one of the simplest types of inviscid flows having the basic features of a three-dimensional flow. A flowfield is classified as conical when all the physical properties, viz., the pressure, density, velocity, and entropy, remain constant along every straight line through a given point called the apex. Conical flows occur, for example, around finite cones in supersonic flows because of the law of forbidden signals. The topological features of conical flow can be understood easily by studying the cross-flow streamlines; i.e., the traces of the conical stream surface's intersection with a sphere, as sketched in Fig. 1. The cross-flow streamlines will have critical points where the cross-flow velocities vanish. For a special class of critical points one can derive rules for the number of these points using Poincare indices. Thus, for example, irrotational conical flows must have an equal number of saddle points and nodes. At a nodal point the entropy, density, and radial velocity are multivalued. At high angles of attack conical streamline patterns exhibit certain global changes such as the liftoff of the leeward node and, perhaps, the appearance of spiral nodes. In addition, the cross flow may become supersonic as it expands about the leading edge, leading to an embedded supersonic cross-flow region terminated by a shock wave (see Fig. 1). It is interesting to note that the perturbation of shock-free flows remains to be studied for conical flows to see if neighboring solutions exist in the classical sense of Morawetz.[2]

The isentropic assumption retains all of the topological features of these flows except spiral nodes and should provide an adequate approximation to the quantitative flow features if the Mach number normal to any shock is less than about 1.4. This approximation greatly simplifies the computations because the governing equation is scalar and the possibility of multiple values at a nodal point (the vortical singularity) is eliminated.

First major success in computing nonlinear irrotational conical flows was reported by Grossman,[3] who devised a quasilinear finite difference method for this problem. An alternative approach is to extend Jameson's[4] finite difference algorithm for transonic full potential equation in the Euclidean three space as a marching scheme to treat supersonic potential flows. This extension has been developed by Shankar[5] using Steger's and Caradona's[6] density linearization technique.

In this paper the theory of irrotational conical flows is described in a general coordinate system defined on a unit sphere. A finite area method is described that represents an extension of the conventional finite volume methods[7,8] to vector fields defined on a curved surface. It is then used to compute various conical flowfields studied by other investigators.[3,9,10] Similarity between the highest order terms of the partial differential equation describing conical flows and that describing plane transonic flows has been exploited to devise a suitable artificial viscosity to implement the (mathematical) entropy condition[11] as well as the construct a stable iteration scheme.

## Cross-Flow Velocity Field

It is essential in the application of the finite area method to frame the equations in an invariant coordinate system. This has been done by first projecting the Euler equations for a general three-dimensional flow onto a sphere of radius $r$, and then scaling them to obtain the description on the unit sphere. We first note that the mainstream velocity components, $Q^i$, and their projection on the sphere of radius $r$, $\tilde{V}^\alpha$, are related by

$$\tilde{V}^\alpha = B^\alpha_i Q^i$$

where

$$B^i_\alpha = \frac{\partial X^i}{\partial \Xi^\alpha}, \qquad \alpha = 1,2 \quad \text{and} \quad i = 1,2,3$$

are the projection factors[12] (or the tangents). Here $X^i$ are coordinates in Euclidian three space and $\Xi^\alpha$ are parametric coordinates on the surface of a sphere. We could also decompose the mainstream velocity as

$$Q^i = B^i_\alpha \tilde{V}^\alpha + Q_R N^i$$

Presented as Paper 82-0995 at the Third AIAA/ASME Joint Thermophysics, Fluids, Plasma and Heat Transfer Conference, St. Louis, Mo., June 7-11, 1982; submitted Jan. 17, 1983; revision received May 25, 1983. 

*Staff Scientist; formerly Research Assistant, Program in Applied Mathematics and Aerospace and Mechanical Engineering, University of Arizona, Tucson, Ariz. Student Member AIAA.

†Dean, College of Engineering and Applied Science and Professor, Aerospace Engineering Sciences. Fellow AIAA.

where $Q_R$ is the radial velocity and $N^i$ the normal to the spherical surface.

Now, with the conical assumption in mind, we introduce a radial scaling to reduce the variables to those on a unit sphere, viz.,

$$V^\alpha = r\tilde{V}^\alpha, \qquad V_\alpha = \tilde{V}_\alpha / r$$

such that the magnitude of the scaled cross-flow velocity $V^\alpha V_\alpha = \tilde{V}^\alpha \tilde{V}_\alpha = q_c^2$ is independent of $r$. The total velocity is thus

$$Q^i Q_i = Q^2 = q_c^2 + Q_R^2$$

Once the coordinates $\Xi^\alpha$, the metric $g_{\alpha\beta}$, and the velocity vector $V^\alpha$ are defined on a portion of the surface of the unit sphere, we may use elementary results from Riemann geometry to develop the governing equations. For potential flow we need to use only the continuity and energy equations.

The continuity equation for the general three-dimensional inviscid flow is

$$\frac{\partial \rho \sqrt{G} Q^i}{\partial X^i} = 0$$

where $\sqrt{G}$ is determinant of the metric tensor of the space $X^i$, and $\rho$ the gas density. For conical flows this implies that on a unit sphere

$$\frac{\partial \rho \sqrt{g} V^\alpha}{\partial \Xi^\alpha} + 2\rho\sqrt{g} Q_R = 0$$

Here $\sqrt{g}$ is the determinant of the metric tensor of the parametric space $\Xi^\alpha$ on the surface of unit sphere.[13] If the irrotational assumption is made, the velocity $Q^i$ will have a potential $\phi(X^i)$ such that for conical flows

$$\phi(X^i) = rF(\Xi^\alpha)$$

where $F(\Xi^\alpha)$ may be called the conical velocity potential since

$$V_\alpha = \frac{\partial F}{\partial \Xi^\alpha}, \qquad Q_R = F(\Xi^\alpha)$$

We also have the energy equation

$$\rho^{\gamma-1} = 1 + \frac{\gamma - 1}{2} M_\infty^2 (1 - Q^2) \tag{1}$$

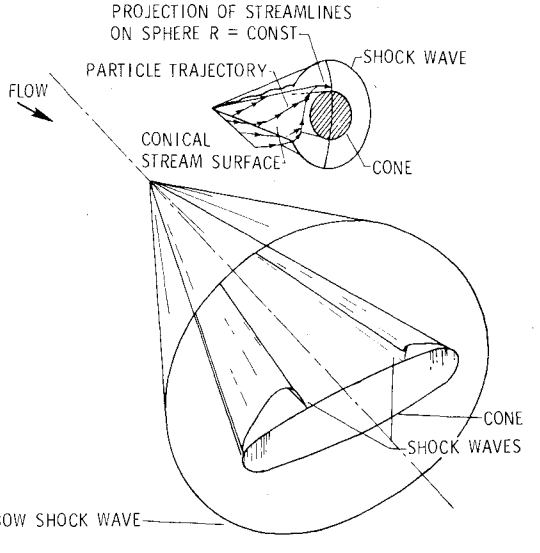


**Fig. 1 Conical flow particle trajectories and stream surface (from Ref. 1), and sketch of flow about an elliptic cone showing bow shock wave, cross-flow sonic surface, and cross-flow shock waves.**

where

$$Q^2 = V^\alpha V_\alpha + F^2$$

and $M_\infty$ is the freestream Mach number. Thus, we must solve the equation

$$\frac{\partial \rho \sqrt{g} V^\alpha}{\partial \Xi^\alpha} + 2\rho\sqrt{g} F = 0 \tag{2}$$

where

$$V^\alpha = g^{\alpha\beta} \frac{\partial F}{\partial \Xi^\beta} \tag{3}$$

and the density is given by the energy equation (1).

Substituting Eqs. (1) and (3) into Eq. (2) and performing the differentiation, we find the quasilinear form of the governing partial differential equation:

$$\rho\sqrt{g}\left[\left(g^{\alpha\beta} - \frac{V^\alpha V^\beta}{a^2}\right) V_{\alpha\|\beta} + \left(2 - \frac{q_c^2}{a^2}\right) F\right] = 0 \tag{4}$$

where $\|$ denotes surface convariant differentiation[12] and the sound speed $a$ and is given by

$$a^2 M_\infty^2 = \rho^{\gamma-1} \tag{5}$$

Equation (4) changes its type when

$$\left(g^{12} - \frac{UV}{a^2}\right)^2 - \left(g^{11} - \frac{U^2}{a^2}\right)\left(g^{22} - \frac{V^2}{a^2}\right) = 0$$

or, noting $g > 0$ always, when

$$\frac{1}{g}\left[\frac{q_c^2}{a^2} - 1\right] = 0$$

Here we use the notation

$$V^\alpha = \begin{pmatrix} U \\ V \end{pmatrix}, \quad V_\alpha = \begin{pmatrix} u \\ v \end{pmatrix}, \quad \text{and} \quad \Xi^\alpha = \begin{pmatrix} \xi \\ \eta \end{pmatrix}$$

Thus, the equation is hyperbolic, parabolic, or elliptic depending on whether the cross-flow Mach number $M_c$ is greater, equal, or less than 1. We could also derive this result by choosing a local coordinate system aligned with the cross-flow streamlines.

If we define streamwise and normal coordinates $s$, $n$ such that

$$V_\alpha \frac{\partial \Xi^\alpha}{\partial n} = 0 \quad \text{and} \quad \epsilon_{\alpha\beta} V^\alpha \frac{\partial \Xi^\beta}{\partial s} = 0$$

with

$$g_{\alpha\beta} \frac{\partial \Xi^\alpha}{\partial s} \frac{\partial \Xi^\beta}{\partial s} = g_{\alpha\beta} \frac{\partial \Xi^\alpha}{\partial n} \frac{\partial \Xi^\beta}{\partial n} = 1$$

Here $\epsilon_{\alpha\beta}$ is the surface permutation symbol.[12] Then we find

$$\frac{\partial \Xi^\alpha}{\partial s} = \frac{V^\alpha}{q_c}, \quad \frac{\partial \xi}{\partial n} = -\frac{1}{\sqrt{g}} \frac{v}{q_c} \quad \text{and} \quad \frac{\partial \eta}{\partial n} = \frac{1}{\sqrt{g}} \frac{u}{q_c}$$

Note also that in these coordinates

$$\frac{\partial F}{\partial s} = \frac{\partial F}{\partial \Xi^\alpha} \frac{\partial \Xi^\alpha}{\partial s} = q_c = \frac{V_\alpha V^\alpha}{q_c}$$

and

$$\frac{\partial F}{\partial n} = \frac{\partial F}{\partial \xi}\left(-\frac{1}{\sqrt{g}} \frac{v}{q_c}\right) + \frac{\partial F}{\partial \eta}\left(\frac{1}{\sqrt{g}} \frac{u}{q_c}\right) = 0$$

Similarly, we also obtain the relations

$$\frac{\partial^2 F}{\partial s^2} = \frac{V^\alpha V^\beta}{q_c^2} \frac{\partial^2 F}{\partial \Xi^\alpha \partial \Xi^\beta} + \dots$$

and

$$\frac{\partial^2 F}{\partial n^2} = \left( g^{\alpha\beta} - \frac{V^\alpha V^\beta}{q_c^2} \right) \frac{\partial^2 F}{\partial \Xi^\alpha \partial \Xi^\beta} + \dots$$

Using these relations we may write the governing partial differential equation as

$$-\frac{\rho\sqrt{g}}{a^2} \left[ (q_c^2 - a^2) \frac{\partial^2 F}{\partial s^2} - a^2 \frac{\partial^2 F}{\partial n^2} \right] + \dots = 0$$

We also note the following structure of this equation. Replacing the expression for $\partial^2 F/\partial s^2$ we obtain

$$-\frac{\rho\sqrt{g}}{a^2} \left[ \mu V^\alpha V^\beta \frac{\partial^2 F}{\partial \Xi^\alpha \partial \Xi^\beta} - a^2 \frac{\partial^2 F}{\partial n^2} \right] + \dots = 0$$

where

$$\mu = 1 - (a^2/q_c^2)$$

Now if we define two functions $\tilde{P}$, $\tilde{Q}$ such that

$$\tilde{P} = \mu\rho \frac{\sqrt{g}}{a^2} \left( U^2 \frac{\partial^2 F}{\partial \xi^2} + UV \frac{\partial^2 F}{\partial \xi \partial \eta} \right)$$

and

$$\tilde{Q} = \mu\rho \frac{\sqrt{g}}{a^2} \left( UV \frac{\partial^2 F}{\partial \xi \partial \eta} + V^2 \frac{\partial^2 F}{\partial \eta^2} \right)$$

then the partial differential equation becomes

$$-(\tilde{P} + \tilde{Q}) + \rho\sqrt{g} \frac{\partial^2 F}{\partial n^2} + \dots = 0$$

This form is useful for explaining the introduction of a conservative artificial viscosity.

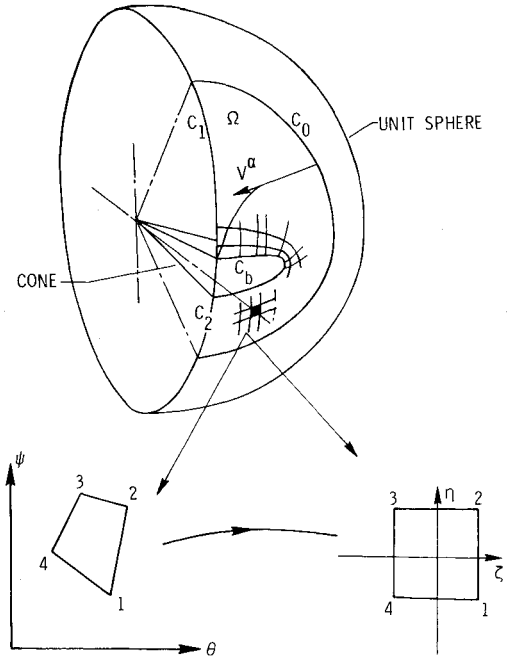


**Fig. 2 The computational domain and a sketch of the bilinear parametric transformation on a unit sphere.**

Finally, we note that the governing equation is of quasilinear type and, hence it admits shock jumps. The jump condition that conserves mass follows immediately from Eq. (2):

$$\left( \frac{d\eta}{d\xi} \right)_{\text{shock}} = \frac{\|\rho V\|}{\|\rho U\|}$$

This is obviously the jump condition that would be desired from the mainstream continuity equation with the conical assumption.

## Finite Area Method

Jameson's finite volume method for the potential equation[8] may be extended to a vector field defined on a non-Euclidian space as long as we have a similar partial differential equation. In this section we develop the finite area method on the unit sphere. It should be emphasized that the derivation would be the same for a vector field on a general curved surface. We assume that on this curved surface a smooth grid is provided, as sketeched in Fig. 2, with the surface coordinates (latitude $\theta$, longitude $\psi$) provided for each nodal point:

$$\theta^\alpha = \begin{pmatrix} \theta \\ \psi \end{pmatrix}$$

We call these primary cells. In order to implement the finite area method the primary cells are mapped to a unit square using a local bilinear transformation in the parametric space, such that

$$\theta = \sum_{i=1}^{4} S^i \theta^i \quad \text{and} \quad \psi = \sum_{i=1}^{4} S^i \psi^i$$

Here $i$ denotes the nodal values and

$$S^i = 4(\tfrac{1}{4} + \xi^i \xi)(\tfrac{1}{4} + \eta^i \eta)$$

The geometrical quantitites are calculated in the following manner. The first fundamental form in the spherical coordinate system $\theta^\alpha$ is $ds^2 = \sin^2\psi d\theta^2 + d\psi^2$, or

$$\tilde{g}_{\alpha\beta} = \begin{bmatrix} \sin^2\psi & 0 \\ 0 & 1 \end{bmatrix} \tag{6}$$

and

$$\sqrt{\tilde{g}} = \sin\psi \tag{7}$$

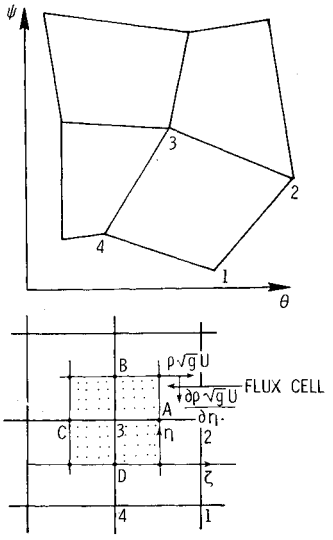


**Fig. 3 Sketch of primary cells and the flux cell.**

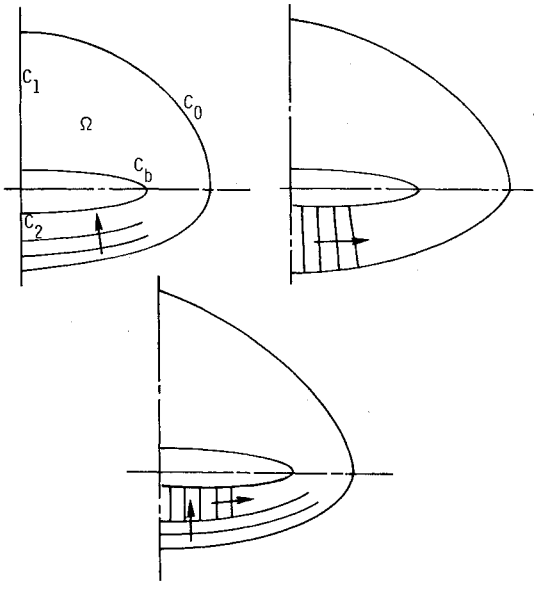


**Fig. 4 Computational boundaries and various possibilities for line relaxation.**

In a mapped coordinate system $\Xi^\alpha$, with $ds^2 = g_{\alpha\beta} d\Xi^\alpha d\Xi^\beta$, then

$$g_{\alpha\beta} = \tilde{g}_{\lambda\mu} \frac{\partial \theta^\lambda}{\partial \Xi^\alpha} \frac{\partial \theta^\mu}{\partial \Xi^\beta} \tag{8}$$

and

$$\sqrt{g} = \sqrt{\tilde{g}} J$$

Here $J$ is the Jacobian of the parametric transformation $\theta^\alpha(\Xi^\beta)$, that is,

$$\sqrt{g} = \sin\psi(\theta_\xi \psi_\eta - \theta_\eta \psi_\xi) \tag{9}$$

We always calculate the geometric quantities at the center of the cells and therefore the bilinear transformation and its best linear substitute have the same role.[14] Thus we take

$$S^i = S^i_b = \tfrac{1}{4} + \xi^i \xi + \eta^i \eta$$

and thus

$$\theta_\xi = \sum_{i=1}^{4} \theta^i \xi^i, \text{ etc.}$$

and at the center of the cell

$$\theta = \frac{1}{4} \sum_{i=1}^{4} \theta^i, \text{ etc.} \tag{10}$$

Equations (6-10) define geometric quantities at the center of primary cells. The flow quantities are also defined at the center of the cells. The potential is of course defined only at the nodal points. The flow quantities may be calculated as follows: Let $f$ be the disturbance to the freestream potential $f_\infty$ due to the body, i.e., $F = f_\infty + f$. Then we assume the disturbed potential also has the bilinear form

$$f = \sum_{i=1}^{4} S^i f^i$$

Because lumping is not used in the present formulation (it was not found to be necessary), we may replace $S^i$ by $S^i_b$. Thus,

$$f = \sum_{i=1}^{4} S^i_b f^i$$

and

$$f_\xi = \sum_{i=1}^{4} \xi^i f^i, \text{ etc.}$$

The total velocity is computed from

$$V^\alpha = g^{\alpha\beta} \left[ \frac{\partial f_\infty}{\partial \Xi^\beta} + \frac{\partial f}{\partial \Xi^\beta} \right]$$

and

$$f_\infty = \cos\hat{\alpha}\cos\psi + \sin\theta\sin\psi\sin\hat{\alpha}$$

where $\hat{\alpha}$ is the angle of attack.

We are now ready to implement the finite area method. We first introduce a secondary interlocking cell structure, as shown in Fig. 3, in order to integrate the mass continuity equations. We now integrate the weak conservation law over the domain $\Omega$ so that

$$\int_\Omega \frac{1}{\sqrt{g}} \frac{\partial \rho \sqrt{g} V^\alpha}{\partial \Xi^\alpha} \sqrt{g} \, d\xi d\eta + \int_\Omega 2\rho F \sqrt{g} \, d\xi d\eta = 0$$

Applying the surface divergence theorem to the first term, we find

$$\int_c \rho \sqrt{g} V^\alpha n_\alpha \, dS + \int_\Omega 2\rho F \sqrt{g} \, d\eta = 0$$

Here $n_\alpha$ is tangent to the surface and normal to the curve $c$. This relation is valid for any arbitrary $\Omega$ and therefore also is valid locally for a flux cell. Since the flux cell faces are parallel to coordinate lines in the mapped plane, and using one-point evaluation for each integral, we obtain

$$\delta[\rho U \sqrt{g}] + \delta[\rho V \sqrt{g}] + (2\rho F \sqrt{g})_0 = 0$$

for each cell, where $\delta[\ \cdot\ ]$ denotes the net flux change across the cell and $0$ the average over the cell. We also need to define the flux quantities at points A, B, C, and D of the flux cell faces. In this formulation we simply use a box scheme to evaluate these terms. Thus we obtain the approximation to Eq. (2) as

$$\mu_\eta \delta_\xi (\rho \sqrt{g} U) + \mu_\xi \delta_\eta (\rho \sqrt{g} V) + \mu_\xi \mu_\eta (2\rho \sqrt{g} F) = 0$$

where $\mu$ and $\delta$ are the averaging and central difference operations, respectively.

#### Boundary Conditions

We consider the computational domain in Fig. 4. The outer boundary $C_0$ is taken well outside the bow shock wave. Boundaries $C_1$ and $C_2$ are symmetry planes and $C_b$ is the cone body where the normal velocity vanishes.

#### Outer Boundary

At the outer boundary all the disturbances vanish, i.e., $f$, $f_\xi$, $f_\eta$ are all zero. This is implemented in the following way: if $N_2$ grids are the rings, then

$$f(I, N_2) = f(I, N_2 + 2) \quad \text{and} \quad f(I, N_2 + 1) = 0$$

#### Symmetry Plane

At the symmetry plane we introduce an additional grid line and explicitly set the reduced potential to be the same on both grid lines. Thus, if $N_1$ grids are in the circumferential direction, then

$$f(1, J) = f(3, J) \quad \text{and} \quad f(N_1 - 1, J) = f(N_1 + 1, J)$$

### Cone Surface

On the body surface the normal velocity should be zero. If $\mathcal{B}(\Xi^\alpha)$ is the cone surface, then $U^i \partial \mathcal{B} / \partial X^i = 0$ implies

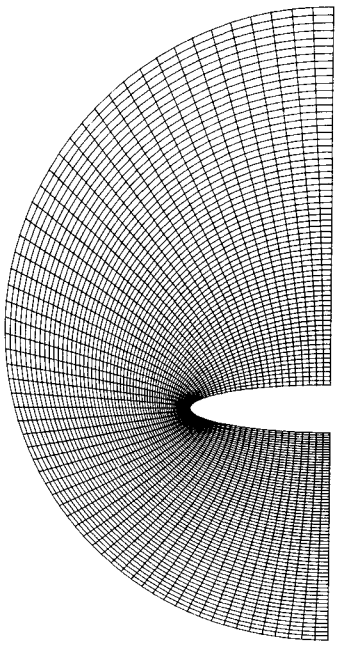

**Fig. 5 The 64×64 mesh for a 18.39:3.17 deg elliptic cone at 10 deg angle of attack.**

$V^\alpha \partial \mathcal{B}/\partial \Xi^\alpha = 0$, since the body is a cone. If the body coincides with a coordinate surface, $\xi$ for example, then $\mathcal{B}(\Xi^\alpha) = \eta = 0$ and the boundary condition implies $V = 0$, i.e., the contravariant cross-flow component that does not lie on the body must vanish. This is implemented by considering a half-flux cell about the cone and using flux reflection.

## Artificial Viscosity

In order to stabilize the scheme in the supersonic regions we desymmetrize the scheme by upwind differencing the contribution for the $F_{ss}$ term. Also, since the higher order terms of the partial differential equation for conical flows are similar to that of plane transonic flows, if we do the upwind differencing with first-order accuracy (at least near the shocks), then the resulting truncation errors will look like the viscous term for plane flows and therefore may be expected to capture any shock waves and insure the entropy condition. The viscosity should be introduced in the conservation form and this can be accomplished in the following manner. Let us consider the case when $V^\alpha > 0$. We noticed earlier that the terms contributing the $F_{ss}$ term have a structure containing $-(\tilde{P}+\tilde{Q})$ and therefore will be evaluated effectively as $-\tilde{P}_{i,j} - \tilde{Q}_{i,j}$ in the finite area scheme. To upwind we need to replace them by $-\tilde{P}_{i-1,j} - \tilde{Q}_{i,j-1}$ and this means we need to add a viscosity term $T_{ij}$, such that $T_{ij} = (\tilde{P}_{i,j} - \tilde{P}_{i-1,j}) + (\tilde{Q}_{i,j} - \tilde{Q}_{i,j-1})$, to the residual $R_{ij}$. We use the switching function

$$\mu = 1 - (a^2/q_c^2) \qquad \text{in the supersonic zones}$$

$$= 0 \qquad \text{in the subsonic zones}$$

The method has to be appropriately modified for the other directions of contravariant velocity.

## Iteration Scheme

The nonlinear algebraic equations resulting from the finite area method are solved using a "constructed" line relaxation scheme. This means that we assume that the problem is being solved by Jameson's special relaxation method.[9] Here we assume that the iteration process is equivalent to a problem of evolution in an artificial time and choose the explicit time-dependent terms such that the problem is well posed. We do have certain restrictions on the direction of the sweep. We should not sweep against the flow inside the supersonic zone. At high angle of attack this condition is difficult to maintain

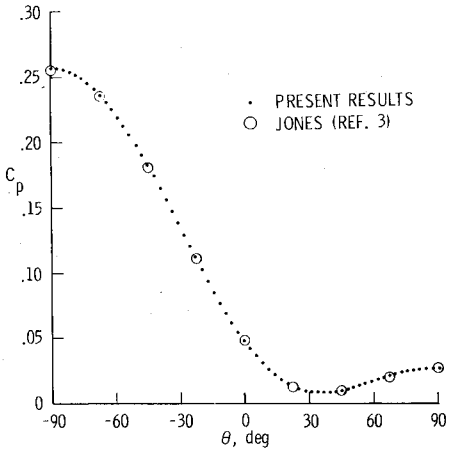


**Fig. 6a Surface distribution for a circular cone at 10 deg angle of attack with $M_\infty = 2.0$; 64×64 grid. Comparison is with the rotational calculations of Jones.[9]**

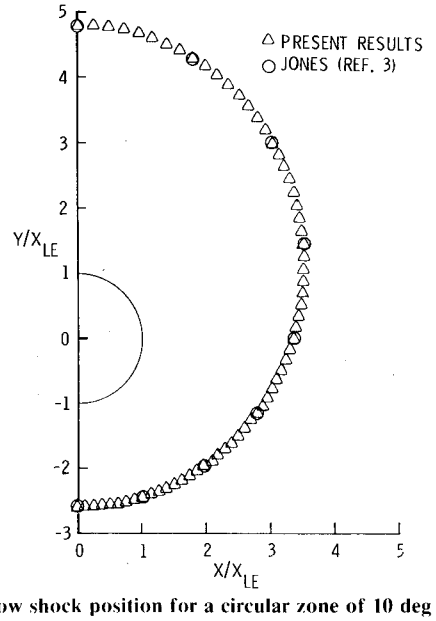


**Fig. 6b Bow shock position for a circular zone of 10 deg half-angle of 10 deg angle of attack. Calculated using a 64×64 grid. Comparison is with the rotational calculations of Jones.[9]**

with a ring relaxation inward from the bow shock wave. Thus the suitable line relaxations are either a circumferential sweep or a combination of the two (see Fig. 4). One should note that the restrictions on the sweep direction can be removed easily by devising an approximate factorization scheme.[16] We use line relaxation mainly to test the finite area formulation. It was found that a circumferential relaxation from windward to leeward is the best in most of the cases and is the scheme described herein. Assume that $V^\alpha > 0$ and consider the line relaxation scheme.

$$A_1 C_{ij} + A_2 (C_{ij} - C_{i-1,j}) + A_3 (C_{ij} - C_{i,j-1}) + A_4 (C_{ij} - C_{i,j+1}) = R_{ij} + T_{ij} + A_5 (C_{i-1,j-1} - C_{i-1,j+1})$$

If we now consider that $R_{ij} + T_{ij}$ are equivalent to their quasilinear finite difference equivalent multiplied by $\rho\sqrt{g}$, then, construction of the Jameson iterative scheme will give the following values for $A_1, \ldots, A_5$:

$$A_1 = \rho\sqrt{g}\left(g^{11} - \frac{U^2}{a^2}\right)\left(\frac{2}{\omega} - 1\right) \qquad \text{subsonic}$$

$$= 0 \qquad \text{supersonic}$$

where $\omega$ is the over-relaxation factor,

$$A_2=\rho\sqrt{g}\left(g^{11}-\frac{U^2}{a^2}+3\mu\frac{U^2}{a^2}+2\mu\frac{UV}{a^2}\right)$$

$$A_3=\rho\sqrt{g}\left(g^{22}-\frac{V^2}{a^2}+3\mu\frac{V^2}{a^2}+2\mu\frac{UV}{a^2}\right)$$

$$A_4=\rho\sqrt{g}\left(g^{22}-\frac{V^2}{a^2}+\mu\frac{V^2}{a^2}\right)$$

and

$$A_5=\frac{1}{2}\rho\sqrt{g}\left(g^{12}-\frac{UV}{a^2}+\mu\frac{UV}{a^2}\right)$$

where $\mu$ is the switching function. We note here that in subsonic flow, provided $\omega<2$, all the coefficients $A_1,\ldots,A_4$ are positive. Thus the scheme is linearly stable. We obtain further insight by looking at its equivalent time-dependent form for each flow type:

Subsonic zone

$$\Delta t\left[\left(g^{11}-\frac{U^2}{a^2}\right)\left(\frac{2}{\omega}-1\right)Ft-\frac{v}{\sqrt{g}q_c}F_{nt}+\frac{U}{q_c}(1-M_c^2)F_{st}\right]=(1-M_c^2)F_{ss}+F_{nn}+\ldots$$

Supersonic zone

$$\Delta t\left[-\frac{v}{\sqrt{g}q_c}F_{nt}-\frac{2(U+V)}{q_c}(1-M_c^2)F_{st}\right]=(1-M_c^2)F_{ss}+F_{nn}+\ldots$$

In the supersonic zone we apply the condition,

$$\left[\frac{U+V}{q_c}(M_c^2-1)\right]^2>\left[\frac{1}{2}\frac{v}{\sqrt{g}q_c}\right]^2(M_c^2-1)$$

to ensure that $s$ is time-like in the unsteady problem as well. This means that

$$4\left(\frac{U+V}{v}\right)^2 g(M_c^2-1)>1$$

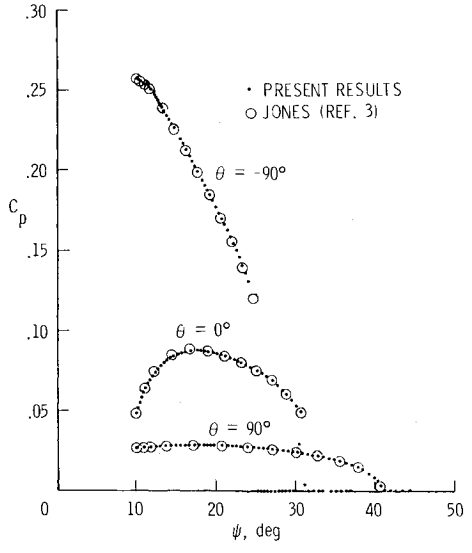


**Fig. 7 Pressure variation between the bow shock wave and the body for a circular cone of 10 deg half-angle at 10 deg angle of attack with $M_\infty=2.0$. Comprison is with the rotational calculations of Jones.[9]**

To ensure that the above condition is always satisfied, especially near the sonic line, we further augment the first term by adding $\epsilon(U+V)F_{st}/q_c$ where $\epsilon$ is as small as possible and yet sufficient to ensure stability. The term $F_{st}$ has to be represented by an upwind difference; we write this as

$$\epsilon\left(\frac{U+V}{q_c}\right)\left[\frac{U}{q_c}(C_{ij}-C_{i-1,j})+\frac{V}{q_c}(C_{ij}-C_{i,j-1})\right]$$

This scheme must be appropriately modified when $V$ changes sign.

## Grid Generation on a Curved Surface

Suppose we are interested in generating grids for a simple connected region on a curved surface. We could use the following simple method: First we note that the first fundamental form in the $\theta^\alpha$ coordinate system is

$$ds^2=g_{\alpha\beta}d\theta^\alpha d\theta^\beta$$

We first transform to a new coordinate system $\Xi^\alpha$ such that

$$ds^2=\lambda^2(d\zeta^2+d\eta^2)$$

where $\lambda=\lambda(\zeta,\eta)$.

This coordinate system is called the isothermal coordinate system[17] and this transform maps the surface portion conformally to a plane. Then we define a complex variable $z$ such that

$$z=\xi+i\eta$$

and apply further conformal transformations to obtain a simple domain where we may generate the desired grids. Alternatively one could derive a numerical grid generation method for the isothermal coordinates. In the present problem we used the grid generation procedure that is commonly used in supersonic computations, that is, we obtain the isothermal coordinates for a unit sphere using stereographic projection and then use a Joukowski transformation followed by a simple shearing to obtain a suitable grid network.

## Results and Discussion

Computations were made to demonstrate that the method predicts qualitative features of simple flows correctly and their quantiative aspects accurately. All the calculations were performed on three mesh levels starting with a $16\times16$ grid

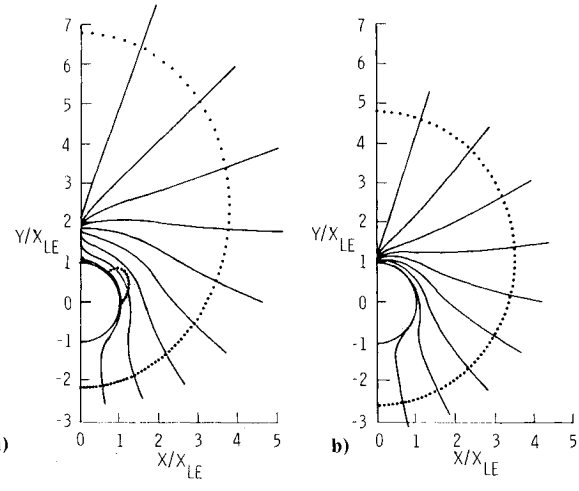


**Fig. 8 Comparisons of the streamline patterns on a circular cone at a) 20 and b) 10 deg angle of attack with $M_\infty=2.0$. Note the liftoff of the leeward node as well as the formation of a supersonic zone in the cross flow.**

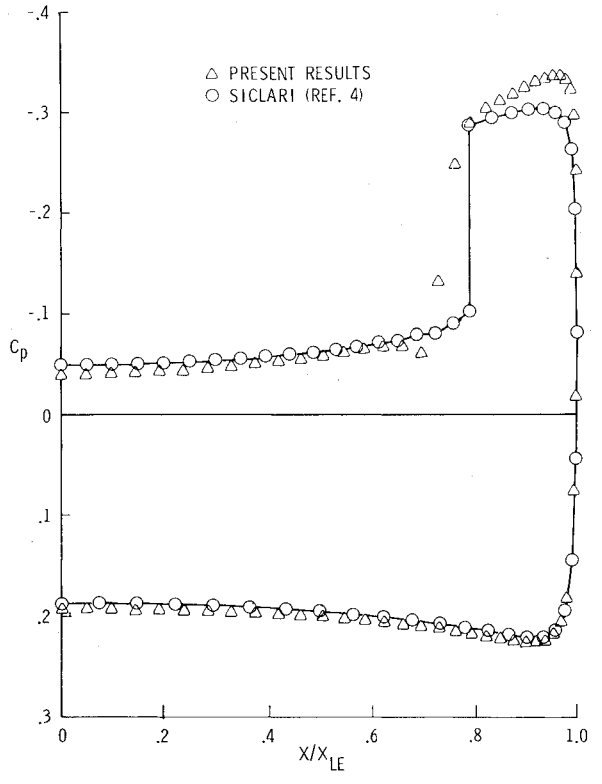


**Fig. 9 Comparison of the results using the Euler equations due to Siclari[10] with the present results for a 18.39:3.17 deg elliptic cone at 10 deg angle of attack with $M_\infty = 1.97$.**

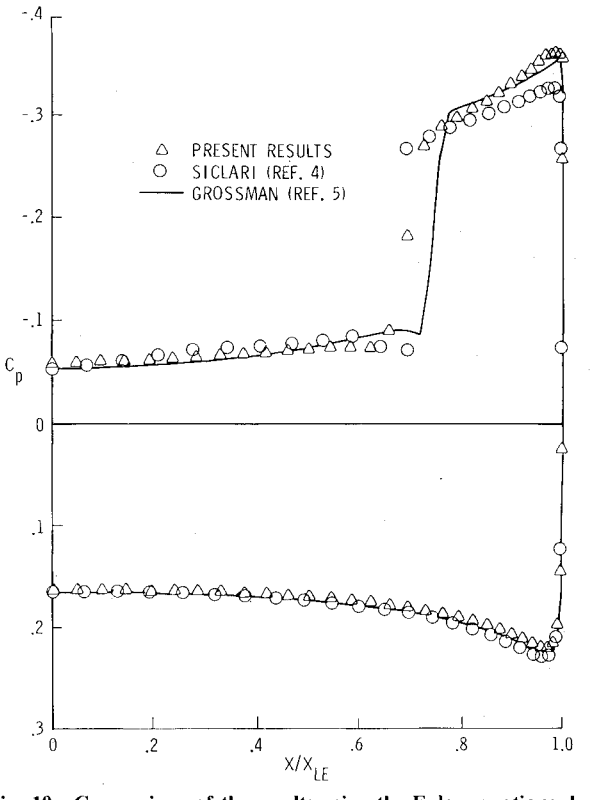


**Fig. 10 Comparison of the results using the Euler equations due to Siclari,[10] and a quasilinear formulation of the potential equation due to Grossman,[13] with the present result for a 20:1.5 deg elliptical cone at 10 deg angle of attack with $M_\infty = 2.0$.**

system. On this initial grid 150 iterations were performed and this was followded by 100 iterations at the $32 \times 32$ level and the final level. Convergence of the last two grids is reliable after 25-50 iterations, depending principally on whether or not there is a body shock wave. Calculations were performed with uniform grids without any clustering; a typical grid is shown in Fig. 5. The results for a circular cone of 10 deg half-angle at 10 deg angle of attack in a freestream of Mach 2, are shown in Figs. 6a and 6b. While the results shown are for a $64 \times 64$ grid, excellent agreement fo the pressure coefficient on the body and the bow shock positions was obtained using the $16 \times 16$ grid, which required fewer than 70 iterations. This coarse grid only requires a few seconds of CDC 7600 CPU time. The pressure distribution in the field is shown in Fig. 7 for three circumferential angles. Excellent with the Euler computations of Jones[9] is again deomonstrated. An example of liftoff is given in Fig. 8 where the streamline patterns for the 10 deg angle-of-attack case are compared with those for an angle of attack of 20 deg.

Results for two thin elliptic cones are shown in Figs. 9 and 10. One ellipse has a major-to-minor axis ratio of approximately 6:1 and the other has a ratio of 13:1. In the first case, a comparison with the Euler equation calculations of Siclari[10] is made. The agreement is generally excellent except for the extra leading-edge suction which may be due, in part, to the potential approximation, and except for the postshock pressure. We note here that the Euler result does not show the expected shock foot singularity‡ captured by our potential calculations. The second example compares the Euler equation results of Siclari, the nonconservative potential finite difference results of Grossman,[3] and our results. Here all three methods capture, to some extent, the shock foot singularity. The finite area method agrees well with the Euler results. The difference in the shock position between the conservative and nonconservative method is to be noted. The total computation time for a case with body shock wave is about 40 s of CDC 7600 CPU time.

‡The pressure gradient immediately behind the shock must be logarithmically infinite.

## Acknowledgments

This research was supported by the Air Force Office of Scientific Research through Grant 81-0107 and the Office of Naval Research through Contract 00014-76-C-0182 and is part of the first author's Ph.D. thesis. Calculations were performed at NASA Ames Research Center using remote facilities supported by NASA Training Grant NGT 03-002-800. The authors wish to thank Drs. M. Salas and K.-Y. Fung for many constructive discussions.

## References

[1] Hayes, W. D. and Probstein, R. F., *Hypersonic Flow Theory*, Vol. 1, Academic Press, New York, 1966, pp. 529-536.

[2] Morawetz, C. S., "The Mathematical Approach to the Sonic Barrier," *Bulletin of the American Mathematical Society*, Vol. 6, No. 2, March 1982, pp. 127-145.

[3] Grossman, B., "Numerical Procedure for the Computation of Irrotational Conical Flows," *AIAA Journal*, Vol. 17, Aug. 1979, pp. 828-837.

[4] Jameson, A., "Transonic Potential Flow Calculations using Conservation Form," *AIAA Second Computational Fluid Dynamics Conference Proceedings*, 1975, pp. 149-155.

[5] Shankar, V., "Conservative Full Potential, Implicit Marching Scheme for Supersonic Flows," *AIAA Journal*, Vol. 20, Nov. 1982, pp. 1508-1514.

[6] Steger, J. L. and Caradona, F. X., "A Conservative Implicit Finite Difference Algorithm for the Unsteady Transonic Full Potential Equation," Flow Simulations, Inc., Sunnyvale, Calif., Rept. 79-04, Dec. 1979.

[7] Rizzi, A. W., "Transonic Solutions of the Euler Equations by the Finite Volume Method," paper presented at the Symposium Transonicum II, Sept. 1975.

[8]Jameson, A. and Caughey, D. A., "A Finite Volume Method for Transonic Potential Flow Calculations," *Proceedings of AIAA 3rd Computation Fluid Dynamics Conference*, Albuquerque, N.M., June 1977, pp. 35-54.

[9]Jones, D. J., "Tables of Inviscid Supersonic Flow about Circular Cones at Incidence, $\gamma = 1.4$," AGARDograph 137, Pt. I, 1969.

[10]Siclari, M. J., "Investigation of Crossflow Shocks on Delta Wings in Supersonic Flow," *AIAA Journal*, Vol. 19, Jan. 1980, pp. 85-93.

[11]Lax, P. D., "Shock Waves and Entropy," *Contributions to Nonlinear Functional Analysis*, Academic Press, New York, 1971, pp. 603-634.

[12]Lovelock, D. and Rund, H., *Tensors, Differential Forms and Variational Principles*, John Wiley & Sons, Inc., New York, 1975.

[13]Sritharan, S. S., "Nonlinear Aerodynamics of Conical Delta Wings," Ph.D. Thesis, University or Arizona, Tucson, Aug. 1982.

[14]Zienkiewicz, O. C., "Why Finite Elements?," *Finite Elements in Fluids*, edited by R. H. Gallagher, J. T. Oden, C. Taylor, and O. C. Zienkiewicz, Vol. 1, John Wiley & Sons, New York, 1978, pp. 1-23.

[15]Jameson, A., "Iterative Solution of Transonic Flows over Airfoils and Wings, Including Flows at Mach 1," *Communications on Pure and Applied Mathematics*, Vol. XXVII, 1974, pp. 283-308.

[16]Holst, T. L., "A Fast, Conservative Algorithm for Solving the Transonic-Potential Equation," AIAA Paper 79-1456, July 1979.

[17]Springer, G., *Introduction to Riemann Surfaces*, Addison-Wesley, Inc., Boston, Mass., 1957, pp. 18-24.